The multiple roles of light-harvesting chlorophyll *a/b*-protein complexes define structure and optimize function of *Arabidopsis* chloroplasts: A study using two chlorophyll *b*-less mutants

Eun-Ha Kim [a], Xiao-Ping Li [b], Reza Razeghifard [a], Jan M. Anderson [a], Krishna K. Niyogi [c], Barry J. Pogson [d], Wah Soon Chow [a,*]

[a] School of Biology, College of Medicine, Biology and Environment, The Australian National University, Canberra, ACT 0200, Australia
[b] Biotechnology Centre for Agriculture and the Environment, Cook College, Rutgers University, New Brunswick, NJ 08901-8520, USA
[c] Department of Plant and Microbial Biology, University of California, Berkeley, CA 94720-3102, USA
[d] ARC Centre of Excellence in Plant Energy Biology, School of Biology, College of Medicine, Biology and Environment, The Australian National University, Canberra, ACT 0200, Australia

ARTICLE INFO

ABSTRACT

The multiple roles of light-harvesting chlorophyll *a/b*-protein complexes in the structure and function of *Arabidopsis* chloroplasts were investigated using two chlorophyll *b*-less mutants grown under metal halide lamps with a significant far-red component. In *ch1-3*, all six light-harvesting proteins of photosystem (PS) II were greatly decreased; in *ch1-3lhcb5*, Lhcb5 was completely absent while the other five proteins were further decreased. The thylakoids of *ch1-3* were less negatively-charged than the wild type, and those of *ch1-3lhcb5* were even less so. Despite the expected weaker electrostatic repulsion, however, thylakoids in leaves of the mutants were not well stacked, an effect we attribute to lower van der Waals attraction, lower electrostatic attraction between opposite charges, and the absence or instability of PSII supercomplexes and peripheral light-harvesting trimers. The quantum yield of oxygen evolution in leaves decreased from 0.109 (wild type) to 0.087 (*ch1-3*) and 0.081 (*ch1-3lhcb5*) O$_2$ (photon absorbed)$^{-1}$; we attribute this decrease to an excessive spillover from PSII to PSI, a limited PSII antenna, and increased light-independent thermal dissipation in PSII in the mutants. Destabilization of the donor side of PSII, indicated by slower electron donation to the redox-active tyrosine Y$_Z^{\cdot}$ in *ch1-3*, probably enhanced PSII susceptibility to photoinactivation, increased the non-functional PSII complexes *in vivo*, and further inactivated PSII complexes *in vitro*. The evolution of chlorophyll *b*-containing chloroplasts seems to fine-tune oxygenic photosynthesis.

© 2009 Elsevier B.V. All rights reserved.

1. Introduction

Higher plant chloroplasts possess highly conserved pigment–protein complexes for the outer light-harvesting antenna of PSI (LHCI) and PSII (LHCII). In PSII, LHCII comprises six major Chl *a/b*-proteins (Lhcb1–6) which non-covalently bind an array of pigments (Chl *a*, Chl *b* and xanthophylls) to form complexes LHCIIb, CP29, CP26 and CP24 [1,2]. The major complex, LHCIIb, is composed of trimeric mixtures of three Lhcb1–3 proteins, products of the *Lhcb1*, *Lhcb2* and *Lhcb3* genes; these trimers bind ~60% of the PSII chlorophyll. Recent studies of the crystal structure of LHCIIb [3,4] found eight molecules of Chl *a*, six Chl *b*, two lutein (Lut), one neoxanthin (Neo) and one of the xanthophyll-cycle carotenoids in each monomer of a LHCIIb trimer. The minor, monomeric complexes, CP29, CP26 and CP24, are formed by the association of pigments with Lhcb4, Lhcb5 and Lhcb6 proteins, respectively. In contrast to LHCIIb, the three proteins Lhcb4, Lhcb5 and Lhcb6 bind ~15% of the Chl molecules, have higher Chl *a/b* ratios and are enriched in violaxanthin (Vio) [5,6]. Trimeric LHCIIb and the monomeric complexes form a large and highly efficient light-harvesting antenna associated with the PSII core reaction centre complex that exists as dimeric LHCII-PSII supercomplexes in the stacked granal membrane domains [7,8].

One useful approach to studying the structure and function of the PSII antenna has been to genetically alter the content of specific pigments, e.g. Chl *b*. Chl *b* is derived from Chl *a* via chlorophyll *a* oxygenase which catalyses oxygenation of the 7-methyl group to a formyl group [9]. A mutation in the chlorophyll *a* oxygenase gene causes loss of Chl *b* synthesis in several *chlorina* mutants such as

barley [10–12] or *Arabidopsis* [13,14], while impairment of Chl *b* synthesis in rice [15] or intermittent-light-grown plants [16,17] leads to either a lack or a reduced amount of LHC proteins in thylakoid membranes. However, the reported levels of the LHCII proteins remaining in mutant species in the absence of Chl *b* are contentious and contradictory. In this study, we re-investigated the levels of the LHCII proteins to relate them to concerted measurements of structure and photosynthetic function in two *Arabidopsis* Chl *b*-less mutants.

In addition to its regulatory roles in light-harvesting, LHCII has been proposed to be required for the stacking of thylakoid membranes, but this is largely circumstantial. It has been observed that decreased levels of LHCIIb in Chl *b*-less mutants such as the *chlorina f2* barley mutant [18] and the *ch-1 Arabidopsis* mutant [13] exhibit fewer stacked thylakoids than wild type. Furthermore, the adhesion properties of isolated thylakoids of barley *chlorina f2* mutant have been altered compared with wild type; restacking requires a higher concentration of Mg^{2+} than for wild type [19,20]. However, some Chl *b*-less mutants may exhibit relatively well stacked thylakoids *in vivo* in spite of loss or deficiency of LHCIIb trimers, suggesting that the abundance of LHCIIb trimers is not the only determining factor for thylakoid stacking. For example, when the main LHCIIb trimers are removed by genetic manipulation, CP26, normally occurring as a monomer, accumulates in larger amounts and forms Lhcb5 trimers [21]. Therefore, we investigated the extent of thylakoid stacking *in vivo* and *in vitro* in our two Chl *b*-less mutants to elucidate various factors that may influence grana formation.

Given that PSII function needs to be regulated and optimized in response to varying irradiance in nature, it is hardly surprising that PSII is dynamically regulated in space and time [22]. The macromolecular organization of LHCII/core PSII supercomplexes within the stacked granal domains ensures that most PSII complexes are not in direct contact with the PSI complexes, which are exclusively located in non-appressed membrane regions, thereby limiting direct energy spillover from PSII to PSI. Moreover, PSII must function under diverse temporal variations in environmental and metabolic factors, particularly the spectral quality and intensity of light. The PSII antenna of higher plants is designed as a highly effective light-harvesting antenna at low irradiance, while under high light, LHCII safely dissipates excess light excitation energy as heat in a heterogeneous non-photochemical process, termed NPQ [23–26].

Studies with Chl *b*-less plants have shown decreased quantum yield of O_2 evolution, decreased photosynthetic capacity [27–32], and increased sensitivity to photoinhibition [29,33], but their causes are not clear [27–33]. Therefore, we aimed to relate the loss of photosynthetic performance to the stoichiometry of the two photosystem reaction centres and their antenna. As for the increased sensitivity to photoinhibition, several factors may play a role. Decreased NPQ in the *chlorina f2* mutant of barley [23,29] supports the hypothesis that NPQ occurs at LHCIIb, but a significant remaining NPQ indicates that there are other dissipation pathways for NPQ [34] including via monomeric LHCII proteins, core antenna proteins of PSII and PsbS [35]. While the decreased NPQ and the associated decrease in photoprotection in Chl *b*-less mutants are consistent with an increased susceptibility to photoinactivation of PSII [23,29,33,34], we investigated other factors that may also contribute to the exacerbation of photoinactivation of PSII.

Here we report on the multiple roles of LHCII in the structure and function of *Arabidopsis* chloroplasts *in vivo* and *in vitro*. We made use of not only the *ch1-3* mutant, but also the *ch1-3lhcb5* mutant, which was produced by crossing the *ch1-3* mutant with the *lhcb5*, an *Arabidopsis* knockout mutant lacking Lhcb5. Although earlier evidence with Chl *b*-deficient mutants pointed to the key role for LHCIIb, here we demonstrate that all LHCII complexes are needed to provide efficient light-harvesting and grana stacking with its associated fine-tuning of photosynthetic function.

2. Materials and methods

Arabidopsis thaliana, cv Columbia-0 wild type, and *ch1-3*, and *ch1-3lhcb5* mutant plants (Fig. 1) were grown in a growth chamber under 200 µmol photons m^{-2} s^{-1} with an 8-h photoperiod at a day/night temperature of 23/18 °C and 60% humidity. The light was supplied by metal halide lamps (MBID250/T/H, Kolorare, Hungary), with a significant far-red component present. *Ch1-3* was kindly provided by Dr. Judy Brusslan [14]. In *Arabidopsis*, *ch1* encodes chlorophyll *a* oxygenase. In *ch1-3* plants there is a 213-bp deletion in the chlorophyll *a* oxygenase gene, resulting in a chlorophyll *b*-less mutant. In order to obtain the *ch1-3lhcb5* double mutant, the *lhcb5* mutant homozygous for a T-DNA insertion in the *LHCB5* gene (obtained from the Salk T-DNA insertion collection) was crossed to *ch1-3*. The F3 generation seeds were grown and PCR screening was conducted only on Chl *b*-less plants (homozygous for the mutant chlorophyll *a* oxygenase gene) to identify lines that were homozygous for *lhcb5*. The *lhcb5* genotype was checked by PCR using two reactions. One reaction amplified the wild type *LHCB5* gene using primers XPL123 (5′-GAGTATGTTCACGTCTAG-GACT-3′) and XPL124 (5′-TTGCTTTACTCTGGTTTAACAC-3′). The second reaction amplified the T-DNA mutant allele using primers LBa1 (5′-TGGTTCACGTAGTGGGCCATCG-3′) and XPL124. After PCR screening the plants that yielded PCR products only from the second reaction were selected and were further checked by immunoblotting to confirm the double mutation. Both mutants were in Columbia-0 background.

2.1. Isolation of thylakoids

Leaves were homogenized in a grinding buffer containing 20 mM Tricine–KOH (pH 8.4), 0.3 M sorbitol, 10 mM EDTA, 10 mM NaHCO$_3$,

Fig. 1. Wild type (left), *ch1-3* (middle) and *ch1-3lhcb5* (right) plants grown in a cabinet under 200 µmol photons m^{-2} s^{-1} for 8 weeks.

5 mM MgCl$_2$, 10 mM KCl, 4.5 mM Na ascorbate and 0.5% BSA. The homogenate was filtered through muslin and centrifuged at 3000 ×g for 2 min at 4 °C. After suspension in 1 ml of 20 mM Tricine–KOH (pH 7.6), 0.3 M sorbitol, 5 mM MgCl$_2$ and 2.5 mM EDTA, the chloroplasts were osmotically shocked in 6 ml of 5 mM MgCl$_2$ for 1 min; then an equal volume of medium was added to give a final concentration of 50 mM HEPES–KOH (pH 7.6), 0.3 M sorbitol, 2.5 mM MgCl$_2$ and 10 mM KCl prior to centrifugation at 3000 ×g for 2 min at 4 °C. Thylakoid membranes were resuspended in a small volume of supernatant and kept on ice in the dark for immediate use or stored at −80 °C. Chl concentrations were determined in buffered 80% acetone according to Porra et al. [36].

2.2. High-performance liquid chromatography (HPLC)

The photosynthetic pigment contents (Chl a, Chl b and carotenoids) were measured by HPLC. Leaf discs were sampled during the light cycle and frozen immediately in liquid nitrogen until pigment extraction. Each leaf disc was ground in 500 μl of acetone:ethyl acetate 3:2 (v/v) and then 400 μl water was added. After centrifugation for 5 min at 13,000 rpm, the upper layer containing pigments was saved and then spun for 3 min at 13,000 rpm [37]. The supernatant (20 μl) was injected and separated by reverse-phase HPLC analysis on a Spherisorb ODS2 5-micron C18 column (Alltech; Columbia, MD) using an ethyl acetate gradient (35 min) in acetonitrile:water:triethylamine 9:1:0.01 (v/v) [38]. Identification of Chl and carotenoids was by retention time relative to known standards at 440 nm and according to absorption spectra for individual peaks with an inline diode array detector (Agilent 1100 series, www.agilent.com), while quantification was by peak area conversion factors obtained with curves of known standards [36,37,39].

2.3. Immunoblotting of LHCII proteins

Thylakoid membranes were washed with a buffer containing 5% sucrose (w/v), 2 mM EDTA and 125 mM Tris–HCl (pH 6.8), centrifuged and resuspended at a Chl concentration of 1.1 mM. An equal volume of a buffer containing 4% SDS (v/v), 28.6 mM β-mercaptoethanol, 5% sucrose, 2 mM EDTA, 0.02% bromophenol blue and 125 mM Tris–HCl (pH 6.8) was added to a suspension of thylakoid membranes. Samples were heated for 5 min at 70 °C, and centrifuged for 5 min at 13,000 rpm. Supernatants were removed and kept at −80 °C until analyses. Proteins were separated on an equal Chl basis for SDS-PAGE using NuPAGE 4–12% Bis–Tris Pre-Cast gels (Invitrogen) and MES-SDS electrophoresis buffer. Separated proteins were electro-transferred onto PVDF membranes (Biorad) by a semi-dryer blotting system (Amersham Biosciences Corp) at 120 mV for 2 h at room temperature. Immunoblotting was performed with anti-LHCII rabbit antibodies obtained from AgriSera (Vannas, Sweden) followed by anti-rabbit IgG linked to horseradish peroxidase (Sigma). Protein bands were detected by Chromogenic methods with 3,3′,5,5′ tetramethylbenzidine liquid substrate system (Sigma).

2.4. Blue-native polyacrylamide gel electrophoresis (BN-PAGE)

Investigation of the supramolecular organization of protein complexes involved in photosynthesis was performed by BN-PAGE [40,41]. The whole procedure was done mainly according to Suora et al. [40] but with slight modifications. Thylakoids were washed with 50 mM BisTris/HCl (pH 7.0) containing 0.33 M sorbitol, sedimented at 2500 ×g for 2 min at 4 °C, and resuspended in 25 mM BisTris/HCl (pH 7.0), containing 20% (w/v) glycerol at 0.7 mg Chl ml^{-1}. An equal volume of resuspension buffer containing 1% (w/v) β-DM was added to the thylakoid suspension. After incubation on ice for 5 min with occasional mixing, insoluble material was removed by centrifugation at 16,000 ×g for 20 min at 4 °C. The supernatant was supplemented with 0.1 volume of sample buffer (100 mM BisTris/HCl, pH 7.0, 0.5 M 6-amino-n-caproic acid, 30% glycerol (w/v) and 5% Serva blue G) and applied to 1.5-mm-thick, 5–15% acrylamide gradient gel. Electrophoresis was performed at 4 °C, 10 mV for 8 h. The cathode buffer containing 0.02% Serva blue G was exchanged with buffer lacking the dye after half of the gel was covered with the dye. The composition of the anode buffer was 50 mM Bis–Tris, pH 7.0 (HCl) and for the cathode buffer, it was 50 mM Tricine, 15 mM Bis–Tris, pH 7.0 (HCl) and 1 M 6-aminocaproic acid.

2.5. Transmission electron microscopy

Leaf fragments were fixed in 4% paraformaldehyde and 2.5% glutaraldehyde in 0.1 M cacodylate buffer containing 10% sucrose for 4 h (first fixation). They were postfixed in 1% osmium tetroxide solution for 2 h (second fixation), and dehydrated in an ascending ethanol series. Samples were washed twice in propylene oxide and then infiltrated in a 50/50 mixture of propylene oxide and Epon-Araldite resin overnight. Samples were then placed in pure Epon-Araldite resin for 8 h and embedded in fresh resin, and incubated at 60 °C overnight. Ultrathin 70–90 nm thick sections were cut with a microtome and then collected on formvar-coated copper grids and stained for 20 min with 6% uranyl acetate and Reinold's lead citrate for 10 min. The sections were examined with a Hitachi H-7100 FA transmission electron microscopy at 75 kV.

2.6. Measurement of the extent of thylakoid stacking in vitro

To measure the variation of the extent of restacking of artificially unstacked thylakoid membranes, chloroplasts (66 μM Chl) were suspended in the dark for 10 min at room temperature in an assay buffer containing 50 mM HEPES–KOH (pH 7.6, 26 mM K$^+$), 300 mM sorbitol and 1 mM EDTA, with or without 20 mM MgCl$_2$. Digitonin assay of thylakoid stacking was performed as described [42]. Thylakoids were treated on ice with digitonin (the ratio of digitonin to Chl was 19:1) for 30 min and buffers were added (7 fold dilution) to stop the action of digitonin. Samples were centrifuged at 10,000 ×g for 10 min at 4 °C and Chl contents of the pellets were determined with buffered 80% acetone [36].

2.7. Estimation of the surface charge density of thylakoid membranes

The net surface charge density of thylakoid membranes was estimated by the release of quenching of 9-aminoacridine (9-AA) fluorescence on adding monovalent or divalent cations [43]. Isolated thylakoids were washed three times in a low-salt medium containing 0.1 M sorbitol, 1 mM EDTA and 10 mM HEPES (pH 7.5 with 5.2 mM KOH) in order to unstack thylakoids, and centrifuged at 1500 ×g for 2 min at 4 °C. They were suspended with the same solution, hereafter called the basic medium, to give a Chl concentration of 1.67 mM. The thylakoid stock was diluted into a low-salt medium containing 0.1 M sorbitol, 1 mM EDTA and 1 mM HEPES (pH 7.6) for measurement. Fluorescence emission from 20 μM 9-AA was measured in the basic media containing thylakoids (11 μM Chl) and 20 μM DCMU, using a SLM-8100 spectrofluorometer (Spectronics, Rochester, NY, USA). The excitation wavelength was 340 nm (band-pass, 4 nm) and the emission peak was at 455±1 nm. MgCl$_2$ or KCl was added to a suspension as small aliquots from stock solutions. After adding each concentration of cations, the suspension was incubated for 2 min with stirring at room temperature in darkness. The maximum fluorescence (F_{max}) was obtained on adding 20 mM MgCl$_2$, and was used to normalize all fluorescence levels.

2.8. Maximum Chl fluorescence of thylakoid suspensions in response to [MgCl$_2$]

Thylakoid membranes were suspended in an assay buffer containing 300 mM sorbitol, 50 mM HEPES–KOH (pH 7.6, 26 mM K$^+$) and a

varied [MgCl$_2$], in a thin cuvette of 1 mm path length and at a Chl concentration of 66 μM. Chl fluorescence was measured with a PAM 101 fluorometer (Heinz Walz, Effeltrich, Germany). The fluorometer was fitted with an ED101 BL emitter/detector that excited fluorescence with blue modulated light and selectively measured the PSII fluorescence in the wavelength range 660–710 nm. A saturation pulse of white light (10,000 μmol photons m^{-2} s^{-1}) was applied in the measurement of F_m.

2.9. Measurements of photosynthetic responses to irradiance

The oxygen evolution rate as a function of irradiance was measured with leaf discs using a gas-phase O$_2$ electrode (Hansatech, King's Lynn, UK) in normal air plus ~1% CO$_2$ [44]. White light intensity was changed by neutral density filters. The quantum yield of oxygen evolution in limiting light was corrected for leaf absorptance α, which was calculated from the Chl content per area (c, μmol m^{-2}) as $\alpha = c/(c+76)$ [45].

The light-saturated uncoupled PSII activity was assayed in a liquid-phase O$_2$ electrode using a medium containing 330 mM sorbitol, 5 mM MgCl$_2$, 10 mM NaCl, 20 mM Tricine (pH 7.6), 5 mM NHCl$_4$ and 0.5 mM phenyl-p-benzoquinone (PpBQ).

2.10. Analysis of the partitioning of excitation energy

Chl fluorescence signals were used to estimate the fraction of absorbed photons utilized in photosynthetic electron transport or thermal dissipation in *Arabidopsis* as described in Hendrickson et al. [46]. Chlorophyll fluorescence yields, F_o (corresponding to open PSII reaction centres) and F_m (corresponding to closed PSII reaction centres) were measured in leaves dark-adapted for 10 min using a PAM 101 fluorometer (Heinz Walz, Effeltrich, Germany) fitted with an ED101 BL emitter/detector that excites fluorescence with blue modulated light and selectively measures the PSII fluorescence in the wavelength range 660–710 nm. The absorbed light was partitioned into the fractions used or dissipated in (1) photochemistry (Φ_{PSII}), (2) light-dependent non-photochemical energy dissipation via processes mediated by a pH gradient or a xanthophyll-cycle (Φ_{NPQ}), and (3) constitutive, light-independent non-photochemical energy dissipation (Φ_D) combined with energy dissipation via fluorescence (Φ_f). Leaves were exposed to limiting actinic light (25 μmol m^{-2} s^{-1}) until the fluorescence reached a steady state, at which a saturating pulse was applied to determine F_m'.

2.11. Quantification of functional PSII and P700

Estimations of oxygen evolution per single-turnover flash, used to monitor the content of functional PSII centres in leaf segments, were made using a leaf disc oxygen electrode with weak background far-red light [47,48]. The estimations are based on the assumption that for every four flashes, four electrons are transferred through each functional PSII, resulting in one O$_2$ molecule being evolved.

Quantification of P700 in isolated thylakoid samples was performed largely as described earlier [49]. Isolated thylakoids were suspended in a buffer containing 400 mM sucrose, 50 mM TES-NaOH (pH 7.5), 10 mM NaCl, 5 mM MgCl$_2$, 1 mM sodium ascorbate, 0.1 mM methyl viologen, 2 μM DCMU and 0.2% (w/v) n-dodecyl-β-D-maltoside (β-DM). The measuring beam at 702 nm was selected by a matched pair of interference filters (full width at half-peak height = 2 nm), one placed at the entrance of a light-tight box, and the other in front of the photomultiplier inside the box. The measuring beam was admitted only shortly before measurement to ensure that the sample was effectively in darkness before actinic illumination. Actinic cross-illumination was with blue-green light selected by a Schott BG 39 filter (~500 μmol photons m^{-2} s^{-1}). Timing of these events and data acquisition was controlled by a pulse/delay generator (Model 555, Berkeley Nucleonics Corporation, USA). A separation of

~15 cm between the cuvette and the photomultiplier helped to minimize chlorophyll fluorescence contamination, which was subtracted from the total signal. Only one actinic flash (0.5 s duration) was given to each sample. An extinction coefficient of 64 mM^{-1} cm^{-1} for P700 (reduced *minus* oxidized) was used calculate the P700 content [50].

2.12. Redox kinetics of P700 induced by a flash in the presence of steady far-red light, and estimation of the antenna size of PSI

Redox changes of P700 in leaf segments were observed with a dual wavelength (820/870 nm) unit (ED-P700DW) attached to a pulse amplitude modulation fluorometer (Walz, Effeltrich, Germany) used in the reflectance mode [51b]. To measure the [P700$^+$] as a fraction of the total P700 during illumination with far-red light, leaf segments were illuminated for >10 s to steady state by a light-emitting diode (~15 μmol photons m^{-2} s^{-1}, peak wavelength 727 nm). Then a single-turnover xenon flash (XST 103 xenon flash) was applied to momentarily photo-oxidize the remaining P700. Flashes were given at 0.1 Hz, and 16 consecutive signals were digitised, acquired and averaged by a home-written computer program (time constant = 95 μs). The maximum signal immediately after the flash was taken as the total amount of photo-oxidisable P700, and was used to normalize the traces to give the fraction of oxidized P700 at any instant. Thereafter, electrons percolated (with an apparent rate coefficient k_{red}) through the transport chain to P700$^+$, while the steady far-red light oxidized P700 (with an apparent rate coefficient k_{ox}) to the steady state value y_{ss} again. Fitting the time course of [P700$^+$] with the equation

$$\left[\text{P700}^+ \right] = \exp(-k_{red}t) + y_{ss}[1 - \exp(-k_{ox}t)]$$

gave the rate coefficient k_{ox} which, at constant far-red light, indicates the relative antenna size off PSI.

2.13. EPR measurements

EPR measurements on thylakoid suspensions (Chl concentration of 1.6 mM for the wild type and 1.0 mM for the *ch1-3* mutant) were carried out using a Bruker ESP 300E spectrometer equipped with a TM011 cavity [51a] to determine the Y$_Z^{\cdot}$ (redox-active tyrosine Z radical) re-reduction kinetics. Saturating 10-μs xenon flashes from an EG&G electro-optic flash lamp focused through a non-magnetic optical fibre were used to excite the sample. The ESP 300E spectrometer computer controlled data acquisition and triggering. The flash lamp was triggered with a fixed delay time after data acquisition had started. The Y$_Z^{\cdot}$ decay kinetic measurements were performed at room temperature in the presence of 2 mM PpBQ as the electron acceptor. The Y$_Z^{\cdot}$ decay kinetics were averaged over 8000 events. The trace of P700$^+$ obtained by illumination was an average of 800 events, using 10 G modulation amplitude and 10 μs time constant. The magnetic field positions were 3479 and 3488 G for Y$_Z^{\cdot}$ and P700$^+$ decay kinetics, respectively. Four scans were averaged for each Y$_D^{\cdot}$ (redox-active tyrosine D) signal. Other instrumental parameters were as given previously [51a].

2.14. Photoinhibition treatment

To examine the susceptibility of PSII to photoinactivation in the absence of D1 protein repair, leaf discs were vacuum-infiltrated with 1 mM lincomycin, allowed to evaporate off excess inter-cellular water, and floated, adaxial side up, on a 1 mM lincomycin solution kept at 25 °C. Illumination was provided at 1600 μmol photons m^{-2} s^{-1} through a heat reflection filter. Leaf discs were sampled at each time point; after dark adaptation for 10 min, fluorescence yield was measured using a Plant Efficiency Analyser (Hansatech, King's Lynn, UK).

3. Results

3.1. Pigment and protein composition of LHCII

The absence of Chl *b* in *ch1-3* and *ch1-3lhcb5*, confirmed by HPLC (Table 1), reduced the total Chl content per leaf area compared with the wild type. Some differences in the carotenoid composition were also observed between mutants and the wild type. There was a reduction in Neo and Lut in the two mutants on a Chl *a* basis. Neo and Lut are xanthophylls that are preferentially found in LHCII [5,6,52], so their deficiency is expected in the two mutants. In contrast, β-carotene was increased on a Chl *a* basis, while violaxanthin (Vio) was marginally increased compared to wild type. Overall, there was little change in the ratio of total carotenoid to Chl *a*.

To determine the composition of LHCII proteins in *ch1-3* and *ch1-3lhcb5*, immunoblot analyses were performed on isolated thylakoid membranes using antibodies (from AgriSera, Sweden) specific to each LHCII protein (Fig. 2). In *ch1-3*, the levels of Lhcb1, Lhcb2, Lhcb4 and Lhcb6 on an equal Chl *a* basis were all significantly reduced compared to the wild type; in contrast, the levels of Lhcb3 and Lhcb5 were similar and increased, respectively, compared with the wild type. In *ch1-3lhcb5*, however, Lhcb5 was not detectable and the amounts of the other 5 proteins were at even lower levels than observed for *ch1-3*.

3.2. The pigment–protein complexes of PSI and PSII

To study the oligomeric composition of the pigment–protein complexes in the wild type (WT), *ch1-3* and *ch1-3lhcb5*, the complexes were gently released from thylakoids by β-DM and separated by BN-PAGE (Fig. 3). While there was a considerable difference in the pattern of protein complexes between wild type and the two mutants, as previously shown in the Chl *b*-less mutant of barley by non-denaturing Deriphat-PAGE [27], the mutants *ch1-3* and *ch1-3lhcb5* showed a somewhat similar pattern between themselves. In the mutants, the PSII–LHCII supercomplexes (Band 1) and LHCII trimers (Band 5) were not detected. The amount of PSII core dimer (Band 2, bottom arrow) was greatly reduced, while that of PSII core monomer (Band 4) was increased. The PSI complexes of the two mutants (Band 3) migrated farther than PSI–LHCI complexes of wild type (Band 2), implying that the mutants had a smaller antenna size. The faster-migrating PSI complex in the mutants is named (PSI + LHCI) [53] which represents PSI with a reduced antenna size. Two relatively strong bands (top two arrows) were detected in both mutants.

3.3. The structural organization of thylakoid membranes was altered in the Chl b-less mutants: the extent of thylakoid stacking in vivo and in vitro

Fig. 4 shows the chloroplasts in palisade cells of dark-adapted leaves of the wild type, *ch1-3* and *ch1-3lhcb5*. In *ch1-3*, significant stacking of thylakoids *in vivo* was observed (Fig. 4B), while thylakoid

stacking in *ch1-3lhcb5* was greatly decreased, resulting in very long stromal thylakoids (Fig. 4C, D). Chloroplasts of the two mutants contained fewer grana than the wild type, and the total granal cross-sectional area per chloroplast in *ch1-3* and *ch1-3lhcb5* was decreased to 35% and 21% of that in the wild type, respectively (Table 2). However, the cross-sectional area of chloroplasts in *ch1-3* and *ch1-3lhcb5* was also less than that of the wild type. When the cross-sectional granal area was expressed as a percentage of the chloroplast area, it was decreased to 70% and 39% of the wild type in the *ch1-3* mutant and *ch1-3lhcb5* mutant, respectively.

The extent of thylakoid stacking *in vitro* was measured by applying a treatment with the non-ionic detergent, digitonin, to stacked and unstacked thylakoids suspended in a buffer with or without 20 mM MgCl₂, respectively, in order to separate granal fragments from stromal thylakoids [54,55]. The granal fragments were pelleted at 10,000 ×*g* (10 K pellet) while stromal thylakoid vesicles remained in the supernatant. Table 2 shows that the Chl contents of the 10 K pellet in the stacked and unstacked thylakoids of the wild type were 55% and 16% of the total Chl, respectively. In *ch1-3* and *ch1-3lhcb5*, the Chl
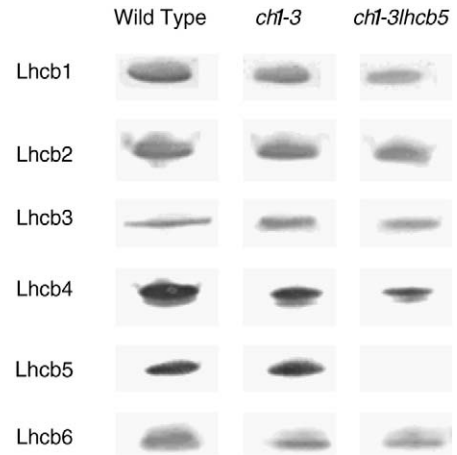

Fig. 2. Immunoblot analysis of LHCII proteins in wild type, *ch1-3* and *ch1-3lhcb5*. Isolated thylakoid membranes from each plant were probed with antibodies specific for the indicated proteins. Each sample contained 2.5 μg Chl *a*.
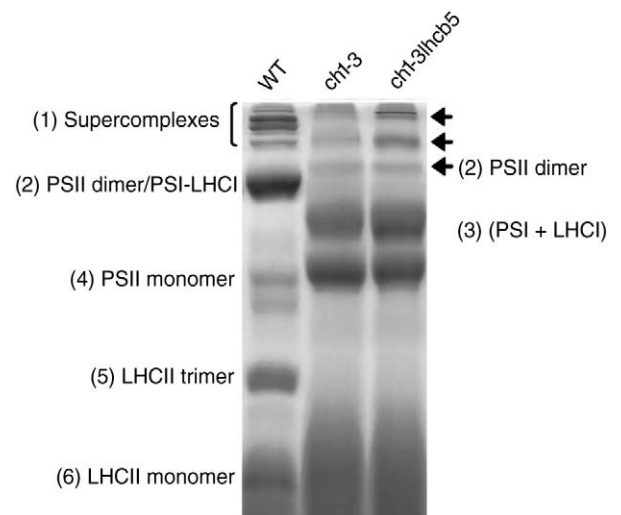

Fig. 3. Analysis of photosynthetic pigment–protein complexes by BN-PAGE of thylakoids from wild type (WT), *ch1-3* and *ch1-3lhcb5*. In each lane, 10 μg Chl was loaded. The gradient of the acrylamide gel was 5–15%. The top two arrows indicate bands of the two mutants that may represent non-specific association of monomeric PSI, while the bottom arrow indicates low-abundance PSII dimers in the mutants. The fast-migrating PSI complex of the mutants named (PSI + LHCI) represents PSI with a reduced antenna size [53].

Table 1
Pigment composition of the wild type, and *ch1-3* and *ch1-3lhcb5* mutants of *Arabidopsis* chloroplasts.

	Wild type	*ch1-3*	*ch1-3lhcb5*
Total Chl [μmol m^{-2}]	480 ± 61	197 ± 12	136 ± 14
Chl *a* [μmol m^{-2}]	361	197 ± 12	136 ± 14
Chl *b* [mmol (mol Chl *a*)$^{-1}$]	330 ± 4	ND	ND
Chl *a*/Chl *b*	3.0	–	–
Neo [mmol (mol Chl *a*)$^{-1}$]	43 ± 1	17 ± 2	17 ± 3
Lut [mmol (mol Chl *a*)$^{-1}$]	217 ± 7	186 ± 21	188 ± 27
β-Car [mmol (mol Chl *a*)$^{-1}$]	136 ± 4	184 ± 11	196 ± 13
Vio [mmol (mol Chl *a*)$^{-1}$]	47 ± 6	58 ± 9	59 ± 23
Total Car [mmol (mol Chl *a*)$^{-1}$]	443 ± 17	445 ± 32	460 ± 35

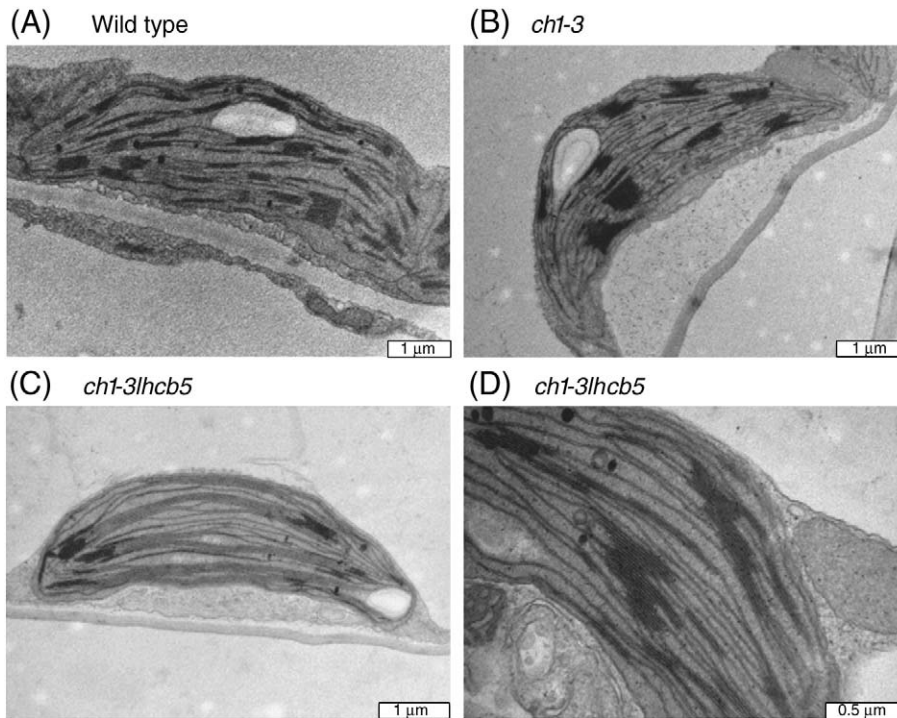Values are means ± SD for four measurements. ND = not detectable.

Fig. 4. Ultrastructure of chloroplasts in palisade cells of fully developed leaves of wild type (A), *ch1-3* (B), and *ch1-3lhcb5* (C and D). The bar represents 1 µm in (A), (B) and (C), but 0.5 µm in (D).

content of the 10 K pellets from the thylakoids suspended in a stacking buffer were 9.4% and 5.5% of total Chl, respectively. These percentages were even lower than that of unstacked thylakoids of wild type, indicating that granal thylakoids were very easily disrupted by digitonin treatment, even in the presence of 20 mM $MgCl_2$.

3.4. Decreased salt-induced rise in the maximum chlorophyll fluorescence yield associated with thylakoid stacking indicates limited thylakoid restacking in the mutants

Thylakoid stacking is associated with a lateral heterogeneous segregation of the two photosystems [56], such that a stacked state corresponds to a high maximum fluorescence yield (F_m) of PSII. The increase of F_m is correlated with the increase in membrane restacking accompanied by a spatial separation of PSI and PSII, thereby restricting the spillover of excitation energy from PSII to PSI [57,58]. To investigate the characteristics of thylakoid stacking by screening of negative membrane surface charges with Mg^{2+} ions, F_m was measured at room temperature as a function of cation concentration added to each suspension of thylakoids. Each F_m at a given concentration of $MgCl_2$ was divided by the F_m of thylakoids suspended in a basic media without $MgCl_2$. Fig. 5 depicts that F_m was markedly increased, as expected, by increasing added [$MgCl_2$] in wild type thylakoids and was saturated at 5 mM. However, the increase in F_m of the thylakoids from ch1-3 and ch1-3lhcb5 was strikingly small even at 20 mM, indicating that the restacking of thylakoid was minimal and thus the lateral segregation of the two photosystems was poorly induced with increasing [$MgCl_2$].

3.5. Estimation of the negative surface charge density of unstacked thylakoids

Limited grana formation in the *ch1-3* and *ch1-3lhcb5* mutants *in vivo* and even poorer grana formation *in vitro* imply that an electrostatic repulsion between two adjacent thylakoids, even in the presence of high concentrations of Mg^{2+}, was not overcome by the attractive forces including van der Waals interaction. Since the electrostatic repulsion between two adjacent membranes depends in part on the surface

charge densities of thylakoid membranes (σ), we estimated σ by 9-AA fluorescence [43]. The magnitude of σ so obtained depends on the level of 9-AA fluorescence between a minimum and maximum, as determined by the salt composition in the buffer. Table 2 shows the surface charge densities obtained at one particular intermediate level of 9-AA fluorescence $F/F_{max} = 0.70$, where F_{max} is the maximum 9-AA fluorescence in a saturating [Mg^{2+}]; thylakoids of *ch1-3* and *ch1-3lhcb5* were about 29% and 33% less negatively-charged, respectively, compared with thylakoids of the wild type. The lower magnitude of σ of thylakoids from the two mutants suggests lower electrostatic repulsion between two adjacent thylakoids.

3.6. The partitioning of energy in PSII and the photosynthetic performance of the mutants relative to the wild type

Absorbed light energy at steady state photosynthesis at a given irradiance can be partitioned into three fractions [46]: (1) that utilized

Table 2
The extent of thylakoid stacking in the wild type and *ch1-3* and *ch1-3lhcb5* mutants of *Arabidopsis* chloroplasts *in vivo* (in leaves) and *in vitro* (in isolated thylakoids), and the surface charge density of thylakoids.

	Wild type	ch1-3	ch1-3lhcb5
in vivo			
Grana per chloroplast	40 ± 3	25 ± 2	19 ± 1
Granal area per chloroplast (µm²)	2.68 ± 0.30	0.95 ± 0.04	0.55 ± 0.03
Chloroplast area (µm²)	15.4 ± 1.7	7.50 ± 0.30	8.40 ± 0.50
Granal area/chloroplast area (%)	17.7 ± 3.3	12.5 ± 0.4	6.9 ± 0.4
in vitro			
Chl in 10 K pellet (%)	54.8 ± 1.3	9.4 ± 1.3	5.5 ± 1.0
Stacking medium (+ 20 mM $MgCl_2$)			
Chl in 10 K pellet (%)	16.4 ± 1.3	4.9 ± 1.0	3.4 ± 1.2
Unstacking medium (− $MgCl_2$)			
Surface charge density (mC m⁻²)	−32.3	−22.8	−21.5

Chl in 10 K pellet is expressed as percentage of the total Chl content in each thylakoid sample.
Values for grana *in vivo* are means ± SD for ≥ 20 chloroplasts, and values for Chl in 10 K pellet are means ± SD for three measurements.
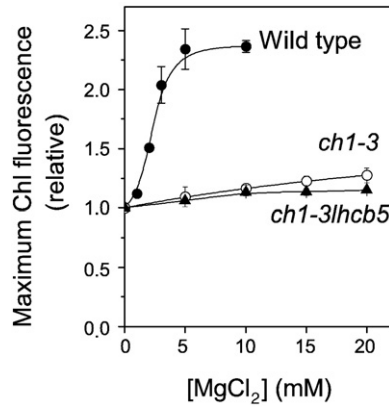
Fig. 5. Response of the maximum chlorophyll fluorescence yield in relative units to $MgCl_2$ concentration added to thylakoid suspensions. Thylakoid membranes of wild type (●), and *ch1-3* (○) and *ch1-3lhcb5* (▲) mutants were suspended in the assay buffer, to which different concentrations of $MgCl_2$ were added. Chl concentration was 66 μM in a thylakoid suspension contained in a cuvette of 1 mm optical path length.

by PSII photochemistry (Φ_{PSII}), (2) that dissipated non-photochemically in light-dependent mechanisms that rely on the light-induced trans-thylakoid pH gradient and the associated xanthophylls cycle (Φ_{NPQ}), and (3) that dissipated as both Chl fluorescence and light-independent quenching ($\Phi_{f,D}$). Φ_{PSII} at limiting irradiance (25 μmol photons $m^{-2} s^{-1}$) decreased in *ch1-3*, and even further in *ch1-3lhcb5* compared with the wild type, while the trend in $\Phi_{f,D}$ was opposite (Table 3).

Associated with the elevated value of $\Phi_{f,D}$ in the two mutants was a lower value of F_v/F_m, a measure of the maximum efficiency of PSII photochemistry in a dark-adapted leaf. F_v/F_m was only 0.66 in *ch1-3lhcb5*, compared with 0.85 in the wild type (Table 3). Consistent with this, the quantum yield of light-limited O_2 evolution was also low in the two mutants (Table 3). The poor photosynthetic efficiency of both mutants relative to the wild type was obviously reflected in their much slower growth (Fig. 1).

To investigate the poor photosynthetic efficiency of both mutants further, the content of functional PSII reaction centres *in vivo* was quantified by the oxygen yield per single-turnover flash given to leaf discs, and that of PSI reaction centres by the P700 content in isolated thylakoids. The content of functional PSII reaction centres *in vivo* and

that of the P700 in isolated thylakoids declined in parallel on a leaf area basis, so that the ratio of functional PSII to PSI was 1.5–1.6 for the wild type and both mutants (Table 3).

The light-saturated uncoupled rate of PSII activity in the presence of an exogenous electron acceptor is directly related to the content of functional PSII complexes in isolated thylakoids. The light-saturated rate of PSII activity, on a P700 basis, was low in *ch1-3*, and even lower in *ch1-3lhcb5* compared with the wild type (Table 3). Interestingly, the light- and CO_2-saturated capacity for O_2 evolution (P_{max}) on a leaf area basis was also decreased in both mutants compared with the wild type.

3.7. EPR spectroscopy of $Y_D^\cdot$, $Y_Z^\cdot$ and $P700^+$ in thylakoid membranes

Fig. 6A shows the room temperature EPR spectra of $Y_D^\cdot$ in thylakoids isolated from the wild type and *ch1-3*, while Figs. 6B and
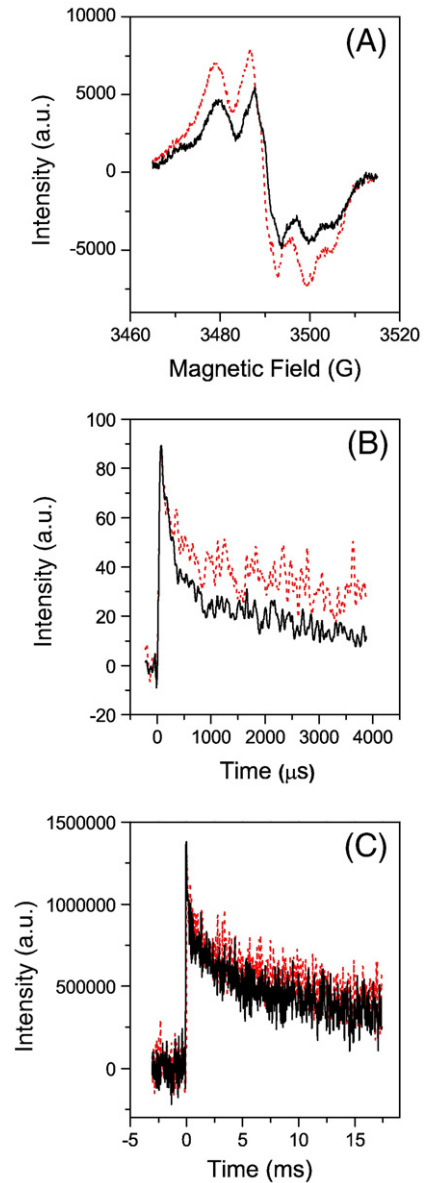

Fig. 6. EPR measurements of $Y_D^\cdot$ spectra and $Y_Z^\cdot$ and $P700^+$ decay kinetics at room temperature in thylakoid membranes from the wild type (solid line) and *ch1-3* (dashed line). (A) $Y_D^\cdot$ spectra, (B) $Y_Z^\cdot$ decay kinetics and (C) $P700^+$ decay kinetics. Spectra were measured with thylakoid suspensions containing 1.5 mM Chl for the wild type, and 1.0 mM Chl for *ch1-3*. Data are uncorrected for different Chl concentrations. Other details are in Materials and methods.

Table 3
Photosynthetic efficiency, capacity, PSI complexes and functional PSII complexes of wild type and *ch1-3* and *ch1-3lhcb5* mutants of *Arabidopsis* chloroplasts *in vivo* and *in vitro*.

	Wild type	*ch1-3*	*ch1-3lhcb5*
Φ_{PSII}	0.80	0.76	0.62
$\Phi_{f,D}$	0.18	0.22	0.33
F_v/F_m	0.846 ± 0.04	0.766 ± 0.03	0.661 ± 0.01
Quantum yield of O_2 evolution [mol O_2 (mol photons)$^{-1}$]	0.109	0.087	0.081
Photosynthetic capacity P_{max} [μmol O_2 $m^{-2} s^{-1}$]	30.4 ± 2.2 (100%)	23.7 ± 4.6 (78%)	23.5 ± 3.0 (77%)
Functional PSII *in vivo* [mmol (mol Chl)$^{-1}$]	2.87 ± 0.50	5.14 ± 0.70	5.73 ± 1.00
[μmol m^{-2}]	1.35 ± 0.10 (100%)	0.99 ± 0.10 (73%)	0.83 ± 0.10 (62%)
P700 *in vitro* [mmol (mol Chl)$^{-1}$]	1.92 ± 0.10	3.23 ± 0.26	3.58 ± 0.10
[μmol m^{-2}]	0.92 ± 0.17 (100%)	0.64 ± 0.09 (69%)	0.49 ± 0.07 (53%)
Functional PSII *in vivo*/P700	1.49 ± 0.10	1.59 ± 0.15	1.60 ± 0.07
PSII activity *in vitro* [mol O_2 s^{-1} (mol P700)$^{-1}$]	17.7 ± 1.4 (100%)	8.26 ± 1.19 (47%)	4.83 ± 0.46 (27%)

Data for Φ_{PSII} and $\Phi_{f,D}$ are means for four leaves illuminated at 25 μmol $m^{-2} s^{-1}$, data for F_v/F_m, functional PSII and P_{max} *in vivo* are means $\pm$ SD for ≥ 10 leaves, and data for P700 *in vitro* and PSII activity *in vitro* are means $\pm$ SD for three thylakoid preparations.

Table 4
The relative contents of $Y_D^.$, $Y_Z^.$ and $P700^+$ in isolated thylakoids of wild type and the *ch1-3* mutant of *Arabidopsis*.

	$Y_D^.$	$Y_Z^.$	$Y_Z^. / Y_D^.$	$P700^+$
Ch1-3/wild type	2.54	1.62	0.64	1.57

C depict the re-reduction kinetics of $Y_Z^.$ and $P700^+$, respectively. EPR measurements were done with different concentrations of Chl in the wild type (1.67 mM) and *ch1-3* (1.00 mM). Fig. 6 shows data obtained with the two different concentrations of Chl, while Table 4 summarizes the ratio of *ch1-3* to wild type for the amplitudes of $Y_D^.$, $Y_Z^.$ and $P700^+$ after correction of data for Chl concentration. The $Y_D^.$ signal intensity is directly related to the total number of PSII reaction centres (whether *active* or *inactive* in performing photochemistry) since there is only one Y_D per PSII reaction centre [59]; once oxidized, whether in an active or inactive PSII, $Y_D^.$ is very slowly re-reduced. The shape of the $Y_D^.$ EPR spectrum was not different in wild type and *ch1-3*, but the amplitude of signal on a Chl basis was greater in *ch1-3* than the wild type by a factor of 2.54 (Table 4).

Fig. 6B shows the $Y_Z^.$ kinetic traces: the rise represents the oxidation of Y_Z by the oxidized PSII primary electron donor, $P680^+$, in the sub-microsecond time frame. The amplitude of $Y_Z^.$ in *ch1-3* was increased by 62% compared to the wild type on a Chl basis (Table 4), while it was approximately 64% that of wild type when these values were normalized to the corresponding amplitude of $Y_D^.$ (Table 4). This result suggests that, assuming for simplicity that all PSII reaction centres in the wild type thylakoids were active, only about 64% of total PSII reaction centres were able to produce $Y_Z^.$ in *ch1-3*. In Fig. 6B, the decay of the $Y_Z^.$ signal in *ch1-3*, representing electron donation by the Mn_4Ca cluster to $Y_Z^.$ through S-state transitions, was significantly slower than that in the wild type, suggesting that $Y_Z^.$ reduction during S-state transitions was retarded.

In PSI, the amplitude of the $P700^+$ EPR signal was increased by 57% in the *ch1-3* mutant compared to the wild type on a Chl basis (Table 4), but the decay kinetics of $P700^+$ were not significantly changed (Fig. 6C), suggesting that the kinetics of rapid electron delivery to $P700^+$ was similar to that of the wild type.

3.8. Relative antenna size of PSI

In addition to the effect of Chl *b* deficiency on the abundance of LHCII protein, we also examined the functional antenna size of PSI. The relative antenna size of PSI was indicated by the rate coefficient of oxidation of P700 by steady far-red light when electrons were simultaneously delivered from PSII to $P700^+$ after a flash (Fig. 7). In
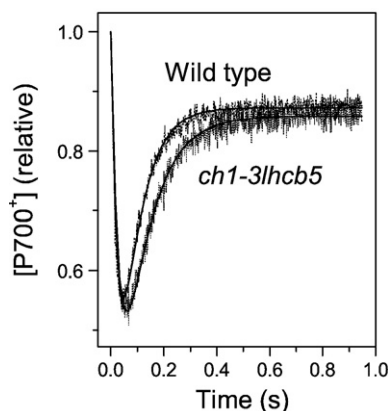

Fig. 7. Redox changes of $[P700^+]$ obtained by applying a single-turnover flash at time 0 in the presence of steady far-red light. Experimental data of wild type and *ch1-3lhcb5* are shown as the upper and lower noisy line, respectively, while fitted curves are smooth solid lines.
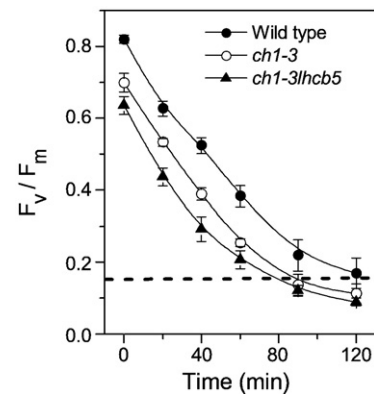

Fig. 8. Photoinactivation of PSII in the wild type, *ch1-3* and *ch1-3lhcb5*. Photosynthetic efficiency of (F_v/F_m) was measured after different durations of photoinhibitory-light exposure (1600 μmol m^{-2} s^{-1}) in the presence of 1 mM lincomycin. The horizontal line indicates a F_v/F_m of 0.15, below which no O_2 was evolved on repetitive flash illumination.

steady far-red light, almost 90% of P700 was oxidized. When a flash was superimposed (at time = 0), the remaining P700 was oxidized to give the maximum signal (magnitude = 1.0) corresponding to complete oxidation of the primary donor. Then electrons percolated (with an apparent rate coefficient k_{red}) through the transport chain to $P700^+$, while the steady far-red light oxidized P700 (with an apparent rate coefficient k_{ox}) to the steady state value y_{ss} again (Fig. 7). Fitting the time course of $[P700^+]$ in Fig. 7 with the equation

$$\left[P700^+\right] = \exp(-k_{red}t) + y_{ss}[1 - \exp(-k_{ox}t)]$$

gave the rate coefficient k_{ox} which at constant far-red light indicates the relative antenna size off PSI. The value of k_{ox} was 13.7 ± 0.3 and 10.4 ± 0.5 s^{-1} for the wild type and the *ch1-3lhcb5* mutant, respectively, showing a decrease by a factor of 1.32 in the mutant.

3.9. Susceptibility of PSII to photoinactivation

Photoinactivation of PSII was measured by a decrease in F_v/F_m in leaves of the wild type, *ch1-3* and *ch1-3lhcb5* after exposure to 1600 μmol m^{-2} s^{-1} in the presence of lincomycin, which prevents the repair of photodamaged PSII reaction centres. In the correlation between F_v/F_m and the fraction of functional PSII measured as an oxygen yield per single-turnover flash in the wild type, photoinhibited leaves having a F_v/F_m value lower than 0.15 (indicated by a horizontal line in Fig. 8) could not evolve oxygen on flash illumination (data not shown). The time of illumination required to reach $F_v/F_m = 0.15$ was longest for the wild type and shortest for *ch1-3lhcb5* (Fig. 8).

4. Discussion

4.1. The absence of Chl b led to a deficiency in total chlorophyll and LHCII proteins per unit leaf area

The most visible effect of the absence of Chl *b* in the two mutants was seen in the pale green leaves which were also much reduced in size (Fig. 1). On a Chl *a* basis, there was some decrease in the levels of LHCII proteins in *ch1-3* thylakoids, namely, Lhcb1, Lhcb2, Lhcb4, and Lhcb6 (Fig. 2). In the *ch1-3lhcb5* mutant, there was a complete loss of Lhcb5, and a further loss of the other LHCII proteins even on a total Chl basis (Fig. 3). Had the gels been loaded on an equal protein basis, the Lhcb bands of the mutants relative to the wild type would have been fainter by a factor of about 2–3, since the effective antenna size of PSII was decreased by a factor of 2.7 and that of PSI by 1.5 (see later).

Immunoblotting analyses of LHC proteins in Chl *b*-less plants including barley, pea, rice and *Arabidopsis* have been reported [14,18,52,60,61]. However, the levels of the LHC proteins remaining

in the absence of Chl *b* are highly variable. In particular, the Chl *b*-less mutants of *Arabidopsis*, ch1-1 and ch1-3, have been suggested to (1) be devoid of the six LHCII proteins in ch1-3 [14], (2) have abundant Lhcb5 and Lhcb3, reduced levels of Lhcb2 and traces of Lhcb1 and Lhcb4 (Fred Smith, AgriSera, personal communication) in ch1-3, or (3) have increased Lhcb5, abundant Lhcb4, reduced levels of Lhcb2 and Lhcb3 and traces of Lhcb1 and Lhcb6 in ch1-1 grown under low light conditions [60]. These discrepancies might be due to the different specificity of antibodies [27], growth stages of plant and/or different growth conditions such as light intensity and quality and temperature [62]. Indeed, studies with the ch1-1 mutant of *Arabidopsis* [60] reveal that the extent of reduction in LHCII proteins is different at high and low light conditions. These authors suggested that the greater decrease in the levels of Lhcb2 and Lhcb3 in ch1-1 under high light as compared with those under low light might be due to enhanced mechanisms for removal of these LHCII proteins under high light which include regulatory proteolysis in the stroma [63] and/or failure in transportation to the chloroplast [64,65].

4.2. The lower levels of all six LHCII proteins in the mutants resulting from the absence of Chl b decreased thylakoid stacking in vivo and in vitro

The extent of thylakoid stacking in leaves was less in *ch1-3* and even less in *ch1-3lhcb5* compared to that of the wild type (Fig. 4, Table 2), confirming that LHCII proteins are important factors for the formation of grana. The complete absence of Lhcb5 in *ch1-3lhcb5*, along with the further loss of the other LHCII proteins compared to wild type, accounts for the much poorer extent of grana formation. Our finding supports the suggestion that Lhcb5 is one factor responsible for thylakoid stacking [21], and for the associated lateral segregation of protein complexes in thylakoids of *chlorina f2* mutant of barley [20]. Indeed, it has been shown that the *asLhcb2 Arabidopsis* mutant lacking Lhcb1 and Lhcb2 (major components of LHCIIb trimers) can form new types of trimeric LHCII from the dramatically increased monomeric Lhcb5, emphasizing the importance of the formation of LHCII trimers in maintaining the oligomeric PSII structure in granal membranes [21,66,67]. Thus, LHCII trimers composed of Lhcb5, Lhcb3 and/or remaining Lhcb2, may help grana formation in *ch1-3*. However, no LHCII trimers were detected in BN-PAGE of *ch1-3* (Fig. 3), which is consistent with green gel data of Chl *b*-less plants including the *ch1-1 Arabidopsis* mutant [13]. Traces of LHCII proteins were found in *ch1-3* at the position corresponding to that of the LHCII trimer in stained BN-PAGE and 2-D BN-SDS-PAGE (data not shown). Either the LHCII trimers (native LHCIIb or composed of Lhcb5 and Lhcb3) could not be formed without Chl *b* or any LHCII trimers in leaves of mutants were easily disrupted in the process of BN-PAGE.

It has been reported that CP24, a complex of Lhcb6 and pigments, acts as a linker for association of one of the LHCIIb trimers to the PSII complex [68]. Each PSII reaction centre is associated with two or four LHCIIb trimers. The dimeric core reaction centre (C_2) forms a highly conserved structural unit (C_2S_2) which consists of two copies each of CP26 and CP29 and two LHCIIb trimers of the S type [8]. Further antenna complexes, two copies of CP24 and two LHCII trimers of the M type, associate with C_2S_2 to give rise to $C_2S_2M_2$ supercomplexes that are predominant in nature [8]. With a drastic decrease in Lhcb6 (normally found in CP24) in *ch1-3* and *ch1-3lhcb5* on a leaf area basis (Fig. 2 lanes obtained with equal Chl *a*, and Table 1 showing the Chl *a* per leaf area), any LHCIIb trimer of the M type present would have been hampered in binding to the PSII complex. PSII monomers, free of their peripheral light-harvesting complexes, were the predominant form observed in the mutants by BN-PAGE (Fig. 3). These PSII monomers could have resulted because either no dimers were present *in vivo*, or that any existing PSII dimers were easily disrupted by the BN-PAGE procedure. Without stable PSII dimers present *in vivo*, and

given the deficiencies of LHCII in the mutants, the extent of thylakoid stacking would have been limited.

The *ch1-3* and *ch1-3lhcb5* mutants had a smaller magnitude of net negative surface charge density (σ) than the wild type (Table 2). Chow et al. [69] proposed that the smaller magnitude of σ in the *chlorina f2* mutant of barley compared with the wild type is due to a lack of LHCIIb proteins, since the proportion of anionic lipids is not changed. Since all 6 LHCII proteins carry net negative charge on their amino acid residues located at the stromal surface, a deficiency of LHCII proteins would be expected to yield a lower magnitude of σ and, therefore, a *lower* electrostatic repulsion which should favour thylakoid stacking. However, the reduced protein mass in LHCII also means markedly lower van der Waals attraction. Chow et al. [69] proposed that a decrease in van der Waals attraction in the *chlorina* barley mutant is responsible for decreased thylakoid stacking, despite a smaller magnitude of σ. In addition, the marked reduction of LHCII proteins around each PSII complex also implies lowering of any *attractive* electrostatic interaction between opposite charges across the partition gap [70]. This may be another reason for the poor extent of thylakoid stacking in both *ch1-3* and *ch1-3lhcb5* mutants.

Nevertheless, the extent of thylakoid stacking in leaf tissue was still moderately substantial even in the *ch1-3lhcb5* mutant relative to stacking *in vitro* (i.e., in isolated thylakoids, Fig. 4 and Table 2). For *in vitro* thylakoids, even when 20 mM $MgCl_2$ was present to lower the electrostatic repulsion, the complete lack of thylakoid stacking (Table 2), coupled with the lack of response of Chl fluorescence to [$MgCl_2$] (Fig. 5), was most striking. Clearly, the environment of the thylakoid membranes is quite different *in vivo* and *in vitro*, and this may have been a factor determining the extent of grana formation *in vitro*, but the mechanism remains to be elucidated.

4.3. The absence of chlorophyll b had a profound effect on photosynthetic efficiency and capacity

It has been established that deficiency in either Chl *b* or some LHCII proteins is not essential for photosynthetic performance [71–73]. However, many studies with Chl *b*-less or Chl *b*-deficient plants including barley and rice have shown that the quantum yield of O_2 evolution and maximum photosynthetic capacity are lower than in wild type plants [29,31,74]. The present study of *ch1-3* and *ch1-3lhcb5* also shows that a deficiency in LHCII is associated with a loss of photochemical efficiency of PSII shown as a reduction of F_v/F_m (Table 3) and Φ_{PSII} in limiting light (Table 3).

At least three factors may contribute to the photochemical inefficiency of PSII in the Chl *b*-less *Arabidopsis*. First, there was less thylakoid stacking in *ch1-3* and *ch1-3lhcb5*, which allowed greater proximity of the two photosystems and enhanced wasteful spillover of excitation energy from PSII to PSI. Spillover, equivalent to quenching of excitation energy in the PSII antenna, would have affected the fluorescence yields of both F_o and F_m in parallel [75,76]. Indeed, Searle et al. [77] reported that the PSII Chl fluorescence lifetime τ_2 (which is directly proportional to the fluorescence yield) for the Chl *b*-less barley mutant was 3.0-fold smaller than that in the wild type when measured in the F_m condition and, similarly, 3.2-fold smaller when measured in the F_o condition. On the basis of the similar proportional decrease in both F_o and F_m, they suggested that increased spillover from PSII to PSI may be one of the factors responsible for the shorter lifetime in the barley mutant. By analogy with the conclusions from the Chl *b*-less mutant of barley and wild type [77], we infer that *ch1-3* and *ch1-3lhcb5* had a larger $\Phi_{f,D}$ than the wild type partly because of greater spillover from PSII to PSI.

Second, there was preferential excitation of PSI relative to PSII, due to depletion of LHCIIb (Fig. 3) as was also shown for the *chlorina f2* mutant of barley [31,72,73]. Both depletion of LHCII and enhanced spillover from PSII to PSI may result in a smaller *effective* antenna size of PSII in the Chl *b*-less mutants. The effective antenna size of PSII,

defined as the effective number of Chl molecules serving each PSII, can be estimated from our results as follows. Taking the example of the wild type, we note that there were 2.87 functional PSII complexes and 1.92 PSI complexes for 1000 total Chl molecules (Table 3). The quantum yield of oxygen evolution was 0.109 mol O_2 (mol photons)$^{-1}$, with a corresponding quantum requirement of 9 photons (mol O_2)$^{-1}$, as compared with a theoretical quantum requirement of 8 photons (mol O_2)$^{-1}$. If we assume that this optimal quantum yield (QY_{max}) is "near perfect", the excitation of both systems must have been balanced. Then half (500) of the 1000 Chl molecules served the 2.87 functional PSII complexes, and 500 served the PSI complexes, giving an effective antenna size of 174 Chl molecules for PSII and 260 for PSI. In the $ch1$-$3lhcb5$ mutant, let n out of 1000 total Chl molecules serve the 5.73 PSII centres; then $(1000 - n)$ Chl molecules served 3.58 PSI centres. Excitation of the two photosystems is balanced when $n = 500$. Deviation of n from 500 gives rise to a lower quantum yield (QY) of oxygen evolution: $n / 500 = QY / QY_{max} = 0.081 / 0.109 = 0.74$, giving $n = 368$, an antenna size of PSII $= 368 / 5.73 = 64$ Chl/PSII, and an antenna size of PSI $= (1000 - n) / 3.58 = 176$ Chl/PSI. Thus the mutations in $ch1$-$3lhcb5$ decreased the effective antenna size of PSII and PSI by a factor of 2.7 and 1.5, respectively. The decrease in the antenna size of PSI was checked by the rate coefficient of oxidation of P700 (k_{ox}) by steady far-red light after electrons had been transferred from PSII to P700$^+$ by a flash; k_{ox} decreased by a factor of 1.32 (Fig. 7), in approximate agreement with the factor of 1.5 estimated above.

A third factor might also have contributed to a greater loss of PSII efficiency in the two mutants as indicated by the reduction in F_v / F_m and Φ_{PSII}, namely, quenching of fluorescence and excitation energy. A comparison of the F_o and F_m value of $ch1$-3 and $ch1$-$3lhcb5$ is revealing. Although both mutants lacked Chl b, they had a somewhat comparable Chl content per unit leaf area so that the magnitude of the fluorescence signal was affected to a similar extent by re-absorption. While F_o was similar for both mutants, F_m (corresponding to closed reaction centre traps) was much decreased in $ch1$-$3lhcb5$ compared with $ch1$-3 (data not shown). This differential decrease in F_o and F_m in $ch1$-$3lhcb5$ could come about if the closed PSII reaction centre in $ch1$-$3lhcb5$ were a stronger fluorescence quencher. For example, it is known that non-radiative losses of the radical pair P680$^+$ Pheophytin$^-$ (probably via charge recombination directly to the ground state) is increased 1000-fold upon closing the PSII reaction centre trap (F_m condition) in wild type pea chloroplasts [78]. To explain the preferential quenching of F_m relative to F_o in $ch1$-$3lhcb5$ (as compared with $ch1$-3), we hypothesize that charge recombination directly to the ground state was more enhanced upon closing the PSII reaction centre in $ch1$-$3lhcb5$.

Interestingly, the light- and CO_2-saturated photosynthetic capacity on a leaf area basis (P_{max}) was decreased in both mutants to about 77% of that in the wild type (Table 3). At light saturation, the antenna size is immaterial, and P_{max} is usually not limited by the content of functional PSII complexes until about half has been inactivated [79]. Since at least 62% of the PSII remained functional in the two mutants on a leaf area basis (Table 3), the decrease in P_{max} must have been due to other factors, such as limitation associated with downstream processes. One possible limitation, yet to be substantiated, is that both mutants were less able to attain a certain redox level in the stroma to activate and optimize CO_2 fixation. Another possibility, which we favour, is that the decreased extent of thylakoid stacking in both mutants failed to allow more space for free diffusion of large stromal enzyme complexes; the consequent crowding due to macromolecules in the stroma would then impair photosynthetic capacity [80].

4.4. Effects on the susceptibility to photoinactivation of PSII

The greater susceptibility of leaves of $ch1$-3 and $ch1$-$3lhcb5$ to photoinactivation of PSII than the wild type (Fig. 8) agrees with a similar finding in a Chl b-less barley mutant [29]. The greater

susceptibility of PSII to photoinactivation in the absence of Chl b might be partly due to the reduced energy-dependent thermal dissipation [81] which protects PSII from damage at very high light intensity [82–84]. Furthermore, an impaired oxidizing side of PSII in $ch1$-3 resulting in slower re-reduction of $Y_Z^·$ (Fig. 6B) would cause the accumulation of the strongly oxidising species P680$^+$ and/or $Y_Z^·$, leading to donor side PSII photoinhibition [85–87]. Harvaux and Tardy [88] demonstrated that LHCII deficiency in the $chlorina$ $f2$ mutant of barley destabilizes the electron donor side of PSII, leading to a higher sensitivity of plants to heat stress, strong light and prolonged dark treatment.

The absence of LHCIIb also destabilized PSII so that on isolation of thylakoids, fewer PSII complexes remained functional. The ratio of functional PSII in vivo to P700 (1.5–1.6) was relatively similar among the wild type and both mutants (Table 3). In contrast, the light-saturated, uncoupled in vitro PSII activity of $ch1$-3 in the presence of an exogenous electron acceptor, expressed on a P700 basis, was only 47% of that of the wild type. This finding shows the fragility of the in vitro PSII complex in the absence of LHCIIb. Indeed, the ratio of ($Y_Z^·$/$Y_D^·$) of $ch1$-3 to that of the wild type was 0.64 in isolated thylakoids (Table 4). Assuming that $Y_Z^·$/$Y_D^·$ was 0.80 in the isolated wild type thylakoids, then $Y_Z^·$/$Y_D^·$ would be 0.51 in $ch1$-3. That is, only about 50% of PSII complexes were capable of oxidizing Y_Z on each flash given to isolated thylakoids of $ch1$-3.

It is uncertain how LHCIIb stabilizes the PSII dimers and maintains the water-splitting complexes in a functional state [88]. Boekema et al. [89] demonstrated that the removal of PsbO and PsbP in spinach induces a shift of strongly-bound LHCIIb trimer and Lhcb4 toward the central part of the supercomplex. Conversely, the removal of LHCII proteins possibly affects the binding affinity or position of extrinsic proteins that stabilize the Mn_4Ca cluster to PSII dimer. Indeed, it was shown that the depletion of LHCII proteins from the PSII super-complexes led to monomerization of PSII supercomplexes [90], with dissociation of the extrinsic protein, PsbO [91]. PSII monomers have lower stability and oxygen evolution rate than PSII–LHCII super-complexes [91–93]. The low ratio of functional PSII to total PSII in vitro ($Y_Z^·$/$Y_D^·$, Table 4) and also the higher in vitro photosensitivity of PSII in $ch1$-3 are probably attributable to the greatly increased abundance of PSII monomers that are incapable of oxidizing $Y_Z^·$. Indeed, Terao et al. [94] concluded that rice mutants with a low Chl b content have photochemically inactive PSII reaction centres which may serve as an antenna for active PSII. Based on this suggestion, $ch1$-$3lhcb5$ with removal of Lhcb5 and reduced LHCII proteins might have had even more severe impairment on the donor side of PSII than $ch1$-3 since LHCIIb does not strongly bind to PSII core complexes without Lhcb5 [95], consistent with the fast photoinactivation observed (Fig. 8).

In conclusion, our present studies with two Chl b-less $Arabidopsis$ mutants, possessing reduced contents of LHCII proteins per PSII, demonstrate that all six LHCII proteins have roles in (1) the balanced excitation of PSII and PSI, (2) stabilization of the structure of PSII supercomplexes, and (3) enhancement of grana formation mainly by increasing the van der Waals attractive force between adjacent thylakoid membranes. Although none of the six Lhcb complexes is strictly required for functionality of PSII core reaction centre complexes, their structural architecture around PSII reaction centre dimers in the $C_2S_2M_2$ mega-complexes help to optimize efficient function of PSII, as well as mitigating the build up of deleterious oxidizing species on the donor side of PSII. In this sense, the evolution of Chl b-containing higher plant chloroplasts fine-tunes oxygenic photosynthesis in ever fluctuating environments.

References

[1] S. Jansson, The light-harvesting chlorophyll a/b binding-proteins, Biochim. Biophys. Acta 1184 (1994) 1–19.

[2] S. Jansson, A guide to the Lhc genes and their relatives in *Arabidopsis*, Trends Plant Sci. 4 (1999) 236–240.

[3] Z. Liu, H. Yan, K. Wang, T. Kuang, J. Zhang, L. Gui, X. An, W. Chang, Crystal structure of spinach major light-harvesting complex at 2.72 Å resolution, Nature 428 (2004) 287–292.

[4] J. Standfuss, A.C.T. Scheltinga, M. Lamborghini, W. Kuhlbrandt, Mechanisms of photoprotection and nonphotochemical quenching in pea light-harvesting complex at 2.5 Å resolution, EMBO J. 24 (2005) 1–10.

[5] R. Bassi, B. Pineau, P. Dainese, J. Marquardt, Carotenoid binding proteins of photosystem II, Eur. J. Biochem. 212 (1993) 297–303.

[6] A.V. Ruban, P.J. Lee, M. Wentworth, A.J. Young, P. Horton, Determination of the stoichiometry and strength of binding of xanthophylls to the photosystem II light harvesting complexes, J. Biol. Chem. 274 (1999) 10458–10465.

[7] E.J. Boekema, J.F.L. Breemen, H. Roon, J.P. Dekker, Arrangement of photosystem II supercomplexes in crystalline macrodomains within the thylakoid membrane of green plant chloroplast, J. Mol. Biol. 301 (2000) 1123–1133.

[8] J.P. Dekker, E. Boekema, Supramolecular organization of thylakoid membrane proteins in green plants, Biochim. Biophys. Acta 1706 (2005) 12–39.

[9] A. Tanaka, H. Ito, R. Tanaka, K. Yoshida, K. Okada, Chlorophyll a oxygenase (CAO) is involved in chlorophyll b formation from chlorophyll a, Proc. Natl. Acad. Sci. U. S. A. 95 (1998) 12719–12723.

[10] D.J. Simpson, O. Machold, G. Hoyer-Hansen, Chlorina mutants of barley (*Hordeum vulgare* L.), Carlsberg Res. Commun. 50 (1985) 223–238.

[11] G. Bellemare, S.G. Barlett, N.-H. Chua, Biosynthesis of chlorophyll a/b-binding polypeptides in wild type and the chlorina f2 mutant of barley, J. Biol. Chem. 257 (1982) 7762–7767.

[12] M.L. Ghirardi, S.W. McCauley, A. Melis, Photochemical apparatus organization in the thylakoid membrane of *Hordeum vulgare* wild type and chlorophyll b-less chlorina f2 mutant, Biochim. Biophys. Acta 851 (1986) 331–339.

[13] D.L. Murray, B.D. Kohorn, Chloroplasts of *Arabidopsis thaliana* homozygous for the ch-1 locus lack chlorophyll b, lack stable LHCPII and have stacked thylakoids, Plant Mol. Biol. 16 (1991) 71–79.

[14] C.E. Espineda, A.S. Linford, D. Devine, J.A. Brusslan, The AtCAO gene, encoding chlorophyll a oxygenase, is required for chlorophyll b synthesis in *Arabidopsis thaliana*, Proc. Natl. Acad. Sci. U. S. A. 96 (1999) 10507–10511.

[15] T. Terao, A. Yamashita, S. Katoh, Chlorophyll b-deficient mutants of rice II. Antenna chlorophyll a/b-proteins of photosystem I and II, Plant Cell Physiol. 26 (1985) 1369–1377.

[16] W.S. Chow, C. Funk, A.B. Hope, Govindjee, Greening of intermittent-light-grown bean plants in continuous light; thylakoids components in relation to photosynthetic performance and capacity for photoprotection, Indian J. Biochem. Biophys. 37 (2000) 395–404.

[17] S.C. Darr, S.C. Somerville, C.J. Arntzen, Monoclonal antibodies to the light-harvesting chlorophyll a/b protein complex of photosystem II, J. Cell Biol. 103 (1986) 733–740.

[18] B. Bossmann, J. Knoetzel, S. Jansson, Screening of chlorina mutants of barley (*Hordeum vulgare* L.) with antibodies against light-harvesting proteins of PSI and PSII: absence of specific antenna proteins, Photosynth. Res. 52 (1997) 127–136.

[19] J.J. Burke, K.E. Steinback, C.J. Arntzen, Analysis of the light-harvesting pigment–protein complex of wild type and a chlorophyll b-less mutant of barley, Plant Physiol. 63 (1979) 237–243.

[20] R. Bassi, U. Hinz, R. Barbato, The role of the light harvesting-complex and photosystem II in thylakoid stacking in the Chlorina-f2 barley mutant, Carlsberg Res. Commun. 50 (1985) 347–367.

[21] A.V. Ruban, M. Wentworth, H. Goodman, A.E. Yakushevska, J. Andersson, P.J. Lee, W. Keegstra, J.P. Dekker, E.J. Boekema, S. Jansson, P. Horton, Plants lacking the main light-harvesting complex retain photosystem II macro-organization, Nature 421 (2003) 648–652.

[22] J.M. Anderson, Strategies of photosynthetic adaptations and acclimation, in: M. Yunus, U. Pathre, P. Monhanty (Eds.), Probing Photosynthesis — Mechanisms, Regulation and Adaptation, Taylor & Francis, London, 2000, pp. 283–292.

[23] P. Horton, A.V. Ruban, R.G. Walters, Regulation of light-harvesting in green plants, Annu. Rev. Plant Physiol. Plant Mol. Biol. 47 (1996) 655–684.

[24] K.K. Niyogi, Photoprotection revisited: genetic and molecular approaches, Annu. Plant Physiol. Plant Mol. Biol. 50 (1999) 333–359.

[25] P. Muller, X.-P. Li, K.K. Niyogi, Non-photochemical quenching. A response to excess light energy, Plant Physiol. 125 (2001) 1558–1566.

[26] P. Horton, A.V. Ruban, Molecular design of the photosystem II light-harvesting antenna: photosynthesis and photoprotection, J. Exp. Bot. 56 (2005) 365–373.

[27] S. Preiss, J.P. Thornber, Stability of the apoproteins of light-harvesting complex I and II during biogenesis of thylakoids in the chlorophyll b-less barley mutant Chlorina f2, Plant Physiol. 107 (1995) 709–717.

[28] Z.-F. Lin, C.-L. Peng, G.-Z. Lin, Z.-Y. Ou, C.-W. Yang, Photosynthetic characteristics of two new chlorophyll b-less rice mutants, Photosynthetica 41 (2003) 61–67.

[29] J.W. Leverenz, G. Öquist, G. Wingsle, Photosynthesis and photoinhibition in leaves of chlorophyll b-less barley in relation to absorbed light, Physiol. Plant. 85 (1992) 495–502.

[30] J. Knoetzel, D.J. Simpson, Expression and organization of antenna proteins in the light- and temperature-sensitive barley mutant chlorina-104, Planta 185 (1991) 111–123.

[31] R. Andrews, M.J. Fryer, N.R. Baker, Consequences of LHC II deficiency for photosynthetic regulation in chlorina mutants of barely, Photosynth. Res. 44 (1995) 81–91.

[32] K.D. Allen, M.E. Duysen, L.A. Staehelin, Biogenesis of thylakoid membranes is controlled by light intensity in the conditional chlorophyll b-deficient CD3 mutant of wheat, J. Cell Biol. 107 (1988) 907–919.

[33] S. Falk, D. Bruce, N.P.A. Huner, Photosynthetic performance and fluorescence in relation to antenna size and absorption cross-sections in rye and barely grown under normal and intermittent light conditions, Photosynth. Res. 42 (1994) 145–155.

[34] A.M. Gilmore, T.L. Hazlett, P.G. Debrunner, Govindjee, Photosystem II chlorophyll a fluorescence lifetimes and intensity are independent of the antenna size differences between barley wild-type and chlorina mutants: photochemical quenching and xanthophyll cycle-dependent nonphotochemical quenching of fluorescence, Photosynth. Res. 48 (1996) 171–187.

[35] N.E. Holt, G.R. Fleming, K.K. Niyogi, Toward an understanding of the mechanism of nonphotochemical quenching in green plants, Biochemistry 43 (2004) 8281–8289.

[36] R.J. Porra, W.A. Thompson, P.E. Kriedemann, Determination of accurate extinction coefficients and simultaneous equations for assaying chlorophylls a and b extracted with four different solvents: verification of the concentration of chlorophyll standards by atomic absorption spectroscopy, Biochim. Biophys. Acta 975 (1989) 394–984.

[37] B. Pogson, K.A. McDonald, M. Truong, G. Britton, D. DellaPenna, *Arabidopsis* carotenoid mutants demonstrates that lutein is not essential for photosynthesis in higher plants, Plant Cell 8 (1996) 1627–1639.

[38] S.R. Norris, T.R. Barrette, D. DellaPenna, Genetic dissection of carotenoid synthesis in *Arabidopsis* defines plastoquinone as an essential component of phytoene desaturation, Plant Cell 7 (1995) 2139–2149.

[39] H. Park, S.S. Kreunen, A.J. Cuttriss, D. DellaPenna, B.J. Pogson, Identification of the carotenoid isomerase provides insight into carotenoid biosynthesis, prolamellar body formation, and photomorphogenesis, Plant Cell 14 (2002) 321–332.

[40] M. Suorsa, R.E. Regel, V. Paakkarinen, N. Battchikova, R.G. Herrmann, E.-M. Aro, Protein assembly of photosystem II and accumulation of subcomplexes in the absence of low molecular mass subunits PsbL and PsbJ, Eur. J. Biochem. 271 (2004) 96–107.

[41] M. Kügler, L. Jänsch, V. Kruft, U.K. Schmitz, H.-P. Braun, Analysis of the chloroplast protein complexes by blue-native polyacrylamide gel electrophoresis (BN-PAGE), Photosynth. Res. 53 (1997) 35–44.

[42] J. Barber, W.S. Chow, C. Scoufflaire, R. Lannoye, The relationship between thylakoid stacking and salt induced chlorophyll fluorescence changes, Biochim. Biophys. Acta 591 (1980) 92–103.

[43] W.S. Chow, J. Barber, Salt-dependent changes of 9-aminoacridine fluorescence as a measure of charge densities of membrane surfaces, J. Biochem. Biophys. Methods 3 (1980) 173–185.

[44] J.R. Evans, The relationship between electron transport components and photosynthetic capacity in pea leaves grown at different irradiances, Aust. J. Plant Physiol. 14 (1987) 157–170.

[45] J. Evans, H. Poorter, Photosynthetic acclimation of plants to growth irradiance: the relative importance of specific leaf area and nitrogen partitioning in maximizing carbon gain, Plant Cell Environ. 24 (2001) 755–767.

[46] L. Hendrickson, R.T. Furbank, W.S. Chow, A simple alternative approach to assessing the fate of absorbed light energy using chlorophyll fluorescence, Photosynth. Res. 82 (2004) 73–81.

[47] W.S. Chow, A.B. Hope, J.M. Anderson, Oxygen per flash from leaf discs quantifies photosystem II, Biochim. Biophys. Acta 973 (1989) 105–108.

[48] W.S. Chow, A.B. Hope, J.M. Anderson, Further studies on quantifying photosystem II in vivo by flash-induced oxygen yield from leaf discs, Aust. J. Plant Physiol. 18 (1991) 397–410.

[49] W.S. Chow, A.B. Hope, The stoichiometries of supramolecular complexes in thylakoid membranes from spinach chloroplasts, Aust. J. Plant Physiol. 14 (1987) 21–28.

[50] T. Hiyama, B. Ke, Difference spectra and extinction coefficients of P700, Biochim. Biophys. Acta 267 (1972) 160–171.

[51] a. E.-H. Kim, R. Razeghifard, J.M. Anderson, W.S. Chow, Multiple sites of retardation of electron transfers in Photosystem II after hydrolysis of phosphatidylglycerol, Photosynth. Res. 93 (2007) 149–158;
    b. W.S. Chow, A.B. Hope, Kinetics of reactions around the cytochrome bf complex studied in intact disks, Photosynth. Res. 81 (2004) 153–163.

[52] B. Bossmann, L.H. Grimme, J. Knoetzel, Protease-stable integration of Lhcb1 into thylakoid membranes is dependent on chlorophyll b in allelic chlorina-f2 mutants of barley (*Hordeum vulgare* L.), Planta 207 (1999) 551–558.

[53] C. Ciambella, P. Roepstorff, E.-M. Aro, L. Zolla, A proteomic approach for investigation of photosynthetic apparatus in plants, Proteomics 5 (2005) 746–757.

[54] W.S. Chow, J.T. Duniec, M.J. Sculley, N.K. Boardman, The stacking of chloroplast thylakoids. Effects of cation screening and binding, studied by the digitonin method, Arch. Biochem. Biophys. 201 (1980) 347–355.

[55] J.H. Argyroudi-Akoyunoglou, S. Kondylaki, G. Akoyunoglou, Growth of grana from "primary" thylakoids in *Phaseolus vulgaris*, Plant Cell Physiol. 17 (1976) 939–954.

[56] B. Andersson, J.M. Anderson, Lateral heterogeneity in the distribution of chlorophyll–protein complexes of the thylakoid membranes of spinach chloroplasts, Biochim. Biophys. Acta 593 (1980) 427–440.

[57] J. Barber, Membrane surface charges and potentials in relation to photosynthesis, Biochim. Biophys. Acta 594 (1980) 253–308.

[58] W.S. Chow, R.C. Ford, J. Barber, Possible effects of the detachment of stromal lamellae from granal stacks on salt-induced changes in spillover, Biochim. Biophys. Acta 635 (1981) 317–326.

[59] W.F.J. Vermaas, A.W. Rutherford, O. Hansson, Site-directed mutagenesis in photosystem II of the cyanobacterium *Synechocystis* sp. PCC 6803: donor D is a tyrosine residue in the D2 protein, Proc. Natl. Acad. Sci. USA 85 (1988) 8477–8481.

[60] R. Tanaka, A. Tanaka, Effects of chlorophyllide a oxygenase overexpression on light acclimation in *Arabidopsis thaliana*, Photosynth. Res. 85 (2005) 327–340.

[61] M. Krol, M.D. Spangfort, N.P.A. Huner, G. Oquist, P. Gustafsson, S. Jansson, Chlorophyll *a/b*-binding proteins, pigment conversions, and early light-harvesting proteins in a chlorophyll *b*-less barley mutant, Plant Physiol. 107 (1995) 873–883.

[62] M. Krol, A.G. Ivanov, S. Jansson, K. Kloppstech, N.P.A. Huner, Greening under high light or cold temperature affects the level of xanthophyll-cycle pigments, early light-inducible proteins, and light-harvesting polypeptides in wild-type barley and the chlorina f2 mutant, Plant Physiol. 120 (1999) 193–204.

[63] M. Lindahl, D.-H. Yang, B. Andersson, Regulatory proteolysis of the major light-harvesting chlorophyll *a/b* protein of photosystem II by a light-induced membrane-associated enzymic system, Eur. J. Biochem. 231 (1995) 503–509.

[64] J.K. Hoober, L.L. Eggink, Assembly of light-harvesting complex II and biogenesis of thylakoid membranes in chloroplasts, Photosynth. Res. 61 (1999) 197–215.

[65] C. Reinbothe, S. Bartsch, L.L. Eggink, J.K. Hoober, J. Brusslan, R. Andrade-Paz, J. Monnet, S. Reinbothe, A role for chlorophyllide a oxygenase in the regulated import and stabilization of light-harvesting chlorophyll *a/b* proteins, Proc. Natl. Acad. Sci. U. S. A. 103 (2006) 4777–4782.

[66] A.V. Ruban, S. Solovieva, P.J. Lee, C. Ilioaia, U. Ganeteg, F. Klimmek, W.S. Chow, J.M. Anderson, S. Jansson, P. Horton, Plasticity in the composition of the light-harvesting antenna of higher plants preserves structural integrity and biological function, J. Biol. Chem. 281 (2006) 14981–14990.

[67] J. Andersson, M. Wentworth, R.G. Walters, C.A. Howard, A.V. Ruban, P. Horton, S. Jansson, Absence of the Lhcb1 and Lhcb2 proteins of the light-harvesting complex of photosystem II — effects on photosynthesis, grana stacking and fitness, Plant J. 35 (2003) 350–361.

[68] L. Kovács, J. Damkjœr, S. Kereïche, C. Ilioaia, A.V. Ruban, E.J. Boekema, S. Jansson, P. Horton, Lack of the light-harvesting complex CP24 affects the structure and function of the grana membranes of higher plant chloroplasts, Plant Cell 18 (2006) 3106–3120.

[69] W.S. Chow, C. Miller, J.M. Anderson, Surface charges, the heterogeneous lateral distribution of the two photosystems, and thylakoid stacking, Biochim. Biophys. Acta 1057 (1991) 69–77.

[70] W.S. Chow, E.-H. Kim, P. Horton, J.M. Anderson, Granal stacking of thylakoid membranes in higher plant chloroplasts: the physicochemical forces at work and the functional consequences that ensue, Photochem. Photobiol. Sci. 4 (2005) 1081–1090.

[71] T.P. Freeman, M.E. Duysen, N.H. Olson, L.D. Williams, Electron transport and chloroplast ultrastructure of a chlorophyll deficient mutant of wheat, Photosynth. Res. 3 (1982) 179–189.

[72] N.K. Boardman, S.W. Thorne, Studies on a barley mutant lacking chlorophyll *b*, II. Fluorescence properties of isolated chloroplasts, Biochim. Biophys. Acta 153 (1968) 448–458.

[73] N.K. Boardman, H.R. Highkin, Studies on a barley mutant lacking chlorophyll *b* — photochemical activity of isolated chloroplasts, Biochim. Biophys. Acta 126 (1966) 189–199.

[74] T. Terao, S. Katoh, Antenna sizes of photosystem I and photosystem II in chlorophyll *b*-deficient mutants of rice. Evidence for an antenna function of photosystem II reaction centers that are inactive in electron transport, Plant and Cell Physiol. 37 (1996) 307–312.

[75] H. Dau, Molecular mechanisms and quantitative models of variable photosystem II fluorescence, Photochem. Photobiol. 60 (1994) 1–23.

[76] A.M. Gilmore, T.L. Hazlett, Govindjee, Xanthophyll cycle-dependent quenching of photosystem II chlorophyll *a* fluorescence: formation of a quenching complex with a short fluorescence life time, Proc. Natl. Acad. Sci. U. S. A. 92 (1995) 2273–2277.

[77] G.F.W. Searle, C.J. Tredwell, J. Barber, G. Porter, Picosecond time-resolved fluorescence study of chlorophyll organisation and excitation energy distribution in chloroplasts from wild-type barley and a mutant lacking chlorophyll *b*, Biochim. Biophys. Acta 545 (1979) 496–507.

[78] H.-W. Trissl, J. Lavergne, Fluorescence induction from photosystem II: analytical equation for the yield of photochemistry and fluorescence derived from analysis of a model including exciton-radical pair equilibrium and restricted energy transfer between photosynthetic units, Aust. J. Plant Physiol. 22 (1995) 183–193.

[79] H.-Y. Lee, W.S. Chow, Y.-N. Hong, Photoinactivation of photosystem II in leaves of *Capsicum annuum*, Physiol. Plant 105 (1999) 377–384.

[80] E.-H. Kim, W.S. Chow, P. Horton, J.M. Anderson, Entropy-assisted stacking of thylakoid membranes, Biochim. Biophys. Acta 1708 (2005) 187–195.

[81] R. Goss, S. Oroszi, C. Wilhelm, The importance of grana stacking for xanthophyll cycle-dependent NPQ in the thylakoid membranes of higher plants. Physiol. Plant. 131 (2007) 496–507.

[82] K.K. Niyogi, A.R. Grossman, O. Bjorkman, *Arabidopsis* mutants define a central role for the xanthophyll cycle in the regulation of photosynthetic energy conversion, Plant Cell 10 (1998) 1121–1134.

[83] B. Demmig-Adams, W. Adams, Photoprotection and other responses of plants to high light stress, Annu. Rev. Plant Physiol. Plant Mol. Biol. 43 (1992) 599–626.

[84] K.K. Niyogi, O. Bjorkman, A.R. Grossman, The roles of specific xanthophylls in photoprotection, Proc. Natl. Acad. Sci. U. S. A. 94 (1997) 14162–14167.

[85] M. Hakala, I. Tuominen, M. Keranen, T. Tyystjarvi, E. Tyystjarvi, Evidence for the role of the oxygen-evolving manganese complex in photoinhibition of Photosystem II, Biochim. Biophys. Acta 1706 (2005) 68–80.

[86] J. Barber, Molecular basis of the vulnerability of photosystem II to damage by light, Aust. J. Plant Physiol. 22 (1994) 201–208.

[87] J.M. Anderson, Y.-I. Park, W.S. Chow, Unifying model for the photoinactivation of photosystem II in vivo under steady-state photosynthesis, Photosynth. Res. 56 (1998) 1–13.

[88] M. Harvaux, F. Tardy, Thermostability and photostability of photosystem II in leaves of the Chlorina-f2 barley mutant deficient in light-harvesting chlorophyll *a/b* protein complexes, Plant Physiol. 113 (1997) 913–923.

[89] E.J. Boekema, J.F.L. Breemen, H. Roon, J.P. Dekker, Conformational changes in photosystem II supercomplexes upon removal of extrinsic subunits, Biochemistry 39 (2000) 12907–12915.

[90] J.P. Dekker, M. Germano, H. Roon, E.J. Boekema, Photosystem II solubilizes as a monomer by mild detergent treatment of unstacked thylakoid membranes, Photosynth. Res. 72 (2002) 203–210.

[91] G.F. Peter, J.P. Thornber, Biochemical evidence that the higher plant photosystem II core complex is organized as a dimer, Plant Cell Physiol. 32 (1991) 1237–1250.

[92] B. Hankamer, J. Nield, D. Zheleva, E. Boekema, S. Jansson, J. Barber, Isolation and biochemical characterization of monomeric and dimeric photosystem II complexes from spinach and their relevance to the organisation of photosystem II in vivo, Eur. J. Biochem. 243 (1997) 422–429.

[93] R. Danielsson, M. Suorsa, V. Paakkarinen, P.-A. Albertsson, E. Styring, E.-M. Aro, F. Mamedov, Dimeric and monomeric organization of photosystem II: distribution of five distinct complexes in the different domains of the thylakoid membranes, J. Biol. Chem. 281 (2006) 14241–14249.

[94] T. Terao, K. Sonoike, J.-Y. Yamazaki, Y. Kamimura, S. Katoh, Stoichiometries of photosystem I and photosystem II in rice mutants differently deficient in chlorophyll *b*, Plant Cell Physiol. 37 (1996) 299–306.

[95] A.E. Yakushevska, P.E. Jensen, W. Keegstra, H. Roon, H.V. Scheller, E.J. Boekema, J.P. Dekker, Supermolecular organization of photosystem II and its associated light-harvesting antenna in *Arabidopsis thaliana*, Eur. J. Biochem. 268 (2001) 6020–6028.